Gel Filtration Chromatographic Study of Micellar Growth of Polyethylene Glycol Dodecyl Ethers

Noriaki FUNASAKI,* Sakae HADA, and Saburo NEYA
Kyoto Pharmaceutical University, Yamashina-ku, Kyoto 607
(Received February 4, 1989)

The aggregation properties of polyethylene glycol dodecyl ethers ($C_{12}E_n$; n=4, 5, and 8) are investigated with frontal gel (Sephadex G-200 and Sephacryl S-500) filtration chromatography (GFC) at 25 °C. At the trailing boundary of derivative GFC patterns for $C_{12}E_5$, unusual two peaks of micelles appear together with a peak of monomer. These micellar peaks are assigned to two types of micelle, viz., large (R_h=30 nm) and small (R_h=5 nm) micelles. As the $C_{12}E_5$ concentration is increased, the peak height for the large micelle increases more rapidly than that for the small micelle. Analysis of the centroid elution volume data by asymptotic theory reveals that the large micelle is the hexamer of the small micelle. This conclusion is supported by computer simulations of the GFC patterns, based on plate theory. In the derivative pattern of the trailing boundary for $C_{12}E_8$, the micellar peak becomes sharper and shifts to larger elution volume side, with increasing concentration. This pattern is well simulated with the assumption of linear concentration dependence of the micellar elution volume. Micelle size of $C_{12}E_8$ appears to remain constant. For $C_{12}E_4$, which is hydrophobically adsorbed on the gels, huge micelles coexist with a small amount of large micelles (R_h=33 nm).

In spite of the large amount of research that has been carried out by using a number of experimental techniques, it is still a matter of controversy if the aggregation number of nonionic surfactant micelles increases or not with increasing surfactant concentration.[1–17] For polyethylene glycol dodecyl ethers ($C_{12}E_n$) at 25 °C, Tanford et al. reported that micellar growth occurs only at $n \leqq 6$.[1] Hexaethylene glycol dodecyl ether ($C_{12}E_6$) has therefore become one of the most extensively investigated nonionic surfactants.[2] Experimental techniques applied for investigations of pentaethylene glycol ($C_{12}E_5$) and octaethylene glycol ($C_{12}E_8$) dodecyl ethers include static (SLS)[3–8] and dynamic (DLS)[7–9] light scattering, nuclear magnetic resonance (NMR),[8–10] static (SNS)[11,12] and dynamic (DNS)[11] neutron scattering, fluorescence decay (FD),[13] fluorescence quenching (FQ),[13] sedimentation velocity (SV), viscosity (VIS),[1,6] gel filtration chromatography (GFC),[1] electron paramagnetic resonance (EPR),[14,15] vapor pressure osmometry (VPO),[16] and electric birefringence.[17] There is general agreement that the $C_{12}E_8$ micelle little grows at 25 °C, but the contradiction remains unsolved for $C_{12}E_5$. For $C_{12}E_5$, EPR[14] and VPO[16] data were interpreted as showing that the $C_{12}E_5$ micelle remains small independently of concentration, whereas SLS[4,5,8,9] and NMR[8] data suggested that $C_{12}E_5$ micelles are polydisperse and increase with increasing concentration.

Two models for micellar growth have been proposed. One is multiple equilibrium model, which assumes that size of large micelles are highly polydisperse and increases with increasing concentration.[18] The second is secondary aggregation model, which assumes that size of large micelles is almost monodisperse and remains constant independently of concentration.[1,2,8,19] The former model denies the presence of the second critical micelle concentration, whereas the latter predicts it.[19]

The advantage of GFC as well as SV over other techniques is to separate mixtures different in size. For the quantitative analysis of GFC patterns for self-associating systems, the large sample size (frontal) method is generally used.[2,20] The small sample size (zonal) method showed that the $C_{12}E_8$ micelle does not grow with increasing concentration at 25 °C.[1] The $C_{12}E_6$ micelle was investigated by both the zonal and frontal methods. The zonal method showed that this micelle grows.[1] The frontal method showed that small and large micelles coexist in equilibrium with each other.[2]

In this work, we investigate aggregation behavior of $C_{12}E_5$, $C_{12}E_8$, and tetraethylene glycol dodecyl ether ($C_{12}E_4$) by the frontal GFC method at 25 °C. In the derivative elution pattern, only one micellar peak is observed for $C_{12}E_8$, whereas two separate micellar peaks are present for $C_{12}E_5$ and $C_{12}E_4$. These results will be analyzed by the asymptotic and plate theories that we have already developed.[2,20]

Theoretical Basis

Secondary Aggregation Model for Micellar Growth. Multiple equilibrium model, which takes into consideration all aggregated species, will be formally the most comprehensive theory for micelle formation.[18] Secondary aggregation model,[19] which will be described below, may be regarded as a special case of this theory.

A small micelle may be formed from m_1 monomers as follows:

$$\underset{C_1}{m_1 \text{ monomers}} \overset{K_1}{\rightleftarrows} \underset{C_2}{\text{small micelle}} \tag{1}$$

and

$$K_1 = C_2/C_1^{m_1}. \tag{2}$$

A large micelle may be formed by the aggregation of m_2 small micelles:

$$\underset{C_2}{m_2 \text{ small micelles}} \overset{K_2}{\rightleftarrows} \underset{C_3}{\text{large micelle}} \tag{3}$$

and

$$K_2 = C_3/C_2^{m_2}. \tag{4}$$

The total concentration C_0 of surfactant may be written as

$$C_0 = C_1 + C_2 + C_3, \tag{5}$$

where all concentrations are expressed on a monomer basis. When m_1 is very large, we can use the approximation of C_1=cmc.

GFC Patterns for Micellar Systems. According to asymptotic theory,[2,20] the centroid volume V_c is defined as

$$V_c = \int_0^{C_0} V \mathrm{d}C/C_0, \tag{6}$$

where V represents the volume flow through the column since introduction of the sample's leading edge. For the above system, V_c can be written as

$$V_c = (C_1V_1 + C_2V_2 + C_3V_3)/C_0, \tag{7}$$

where V_1, V_2, and V_3 denote the elution volumes of the monomer, the small micelle, and the large micelle, respectively. By using the approximation of C_1=cmc, one can obtain

$$C_2 = [C_0(V_c - V_3) + \mathrm{cmc}(V_3 - V_1)]/(V_2 - V_3) \tag{8}$$

and

$$C_3 = [C_0(V_2 - V_c) + \mathrm{cmc}(V_1 - V_2)]/(V_2 - V_3). \tag{9}$$

By using Eqs. 4, 8, and 9, we can determine m_2 and K_2 from GFC elution volume data.

A gel column may be regarded to consist of n successive plates, and each plate is composed of the stationary gel phase and the mobile aqueous phase. This plate theory has been reported for micellar systems in detail.[20] The void volume V_0 and the number n of plates are required for computer-simulation based on this theory. The derivative elution curve provides more detailed information than the original curve.[2,20] For the above micellar system, the plate theory can simulate the derivative pattern.[2,20]

Experimental

Materials. Homogeneous samples of $C_{12}E_8$, $C_{12}E_5$, and $C_{12}E_4$ were obtained from Nikko Chemicals. The purities of these samples were determined to be 99% or more by a Shimadzu GC-8A gas chromatograph. Sephadex G-200 and Sephacryl S-500 were purchased from Pharmacia Fine Chemicals. Blue dextran used for the determination of the void volume was obtained from Pharmacia. Proteins (Sigma) and beads (Dow Chemical Co.) whose hydrodynamic radii R_h (nm) are known were used for the determination of R_h's of micelles; R_h=1.9 (whale myoglobin type II), R_h=3.5 (bovine serum albumin), R_h=4.6 (yeast alcohol dehydrogenase), R_h=8.5 (thyroglobulin), R_h=10.7 (fibrinogen), and R_h=19 (polystyrene carboxylate modified beads). The ion-exchanged water was twice distilled and degassed before use.

Methods. The four columns shown in Table 1 were used, and the flow rate ($cm^3 h^{-1}$) for each column is 6 (A), 8 (B), 24 (C), and 2.3 (D). The temperature of all columns was controlled at 25±0.2 °C. A sample or eluent was charged with a mini-pump. A large volume of sample over the total gel volume V_t was charged so that a plateau region might appear on the elution curve. Elution was monitored continuously with a refractive index monitor and recorded with a Shimadzu Chromatopac C-R1B data processor, except for column D. For the column D experiments the eluate was collected with a fraction collector and the concentration of $C_{12}E_4$ in each fraction was determined by gas chromatography. The refractive index of surfactant solution showed an approximately linear relationship with concentration. When necessary, a correction was made by using the calibration relationship. The derivative of an elution curve was obtained from slopes at appropriate intervals of V. The experimental procedure of GFC has already been reported in detail.[2]

Computer Simulation. Plate theory was used for simulation of the elution curve and its derivative. The equilibria of micellization and partition of a surfactant between the mobile and stationary phases were assumed to be established instantaneously. The simulation procedure has been reported elsewhere.[2,20]

Results and Discussion

$C_{12}E_5$. The dashed line in Fig. 1a shows a typical elution curve in the trailing boundary region for $C_{12}E_5$ (C_0=1.531 mmol dm^{-3}). Since a large amount of a sample was charged, the concentration of $C_{12}E_5$ in the first plateau region was equal to that of the charged sample. The concentration of $C_{12}E_5$ in the second plateau region is close to the cmc values (mmol dm^{-3}), 0.06[21] and 0.064,[22] as we have already predicted theoretically for micellar systems.[20] The derivative of this elution curve (solid line) shows three maxima and two minima. This pattern is unusual, since all GFC derivative patterns reported up to now have only two maxima due to the monomer and the micelle. The first largest peak (V_{3p}) has an elution volume close to the void volume, and therefore, this may be assigned to a large micelle. The last peak (V_{1p}) has a normal elution volume close to the total volume V_t of column A (Table 1). The second peak (V_{2p}) may be due to a small micelle.

To confirm this unusual result, we carried out a similar experiment on column B. As Fig. 1b shows, a very similar derivative pattern was obtained on column B. The first peak appeared near the void volume of column B (Table 1), and the size and shape of the second peak due to a small micelle are close to those on column A, when the difference in V_t between columns A and B is taken into consideration.

Figure 2 shows the derivative pattern for $C_{12}E_5$ as a function of C_0, obtained on column A. The positions of the three peaks little changed with C_0. The

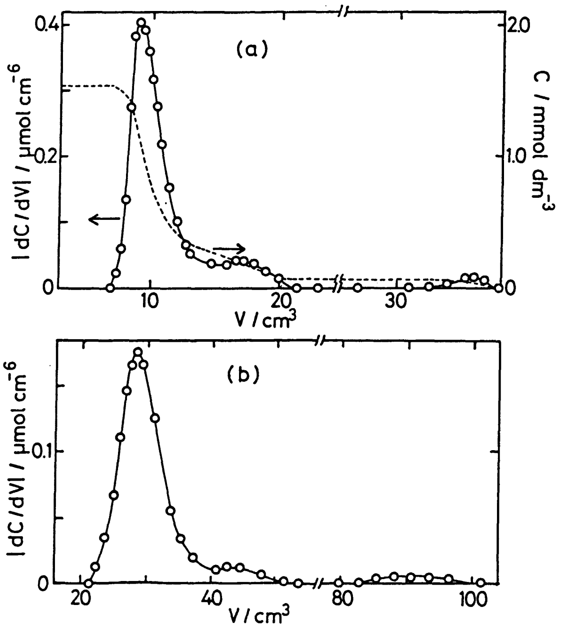

Fig. 1. Elution curve (dashed line) and its derivative (solid line) for $C_{12}E_5$ under two experimental conditions: on column A at C_0=1.5313 mmol dm^{-3} (a) and on column B at C_0=1.530 mmol dm^{-3} (b).

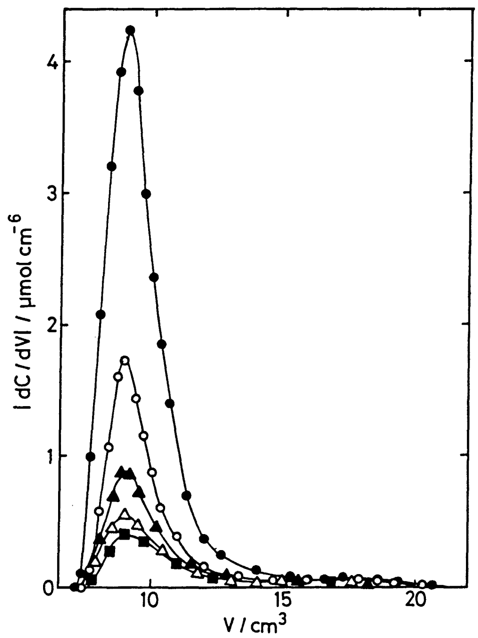

Fig. 2. Derivative elution curves for $C_{12}E_5$ on column A at five charged concentrations (C_0/mmol dm^{-3}): 1.5313 (■); 1.8829 (△); 2.5676 (▲); 4.2537 (○); 10.6343 (●). The monomer region is omitted.

Table 1. Characteristics of the Columns Used

Column	Gel	Total volume (cm^3)	Void volume (cm^3)	Surfactant
A	G-200	30.2	9.5	$C_{12}E_5$
B	G-200	84.4	30.2	$C_{12}E_5$, $C_{12}E_8$
C	S-500	28.9	9.2[a)]	$C_{12}E_4$, $C_{12}E_5$
D	G-200	31.2	9.8	$C_{12}E_4$

a) Estimated as the total volume multiplied by 0.32.

Table 2. Aggregation Numbers and Hydrodynamic Radii of $C_{12}E_5$ Micelles in Dilute Solution at 25 °C

C (mmol dm^{-3})	m	R_h (nm)	Method	Reference
cmc	3270		SLS	4
3.4	3600		SLS	5
cmc	2850	25.2	SLS, NMR	8
7.38		16.2	NMR	9
24.6		28	NMR	10
20%		2.3	EPR	14
cmc	112		VPO	16
		4.9[a)]	GFC	This work
9.82		30[b)]	GFC	This work

a) Estimated from V_2 for the small micelle. b) Estimated from the micellar peak for the large micelle by using column C.

height of the monomer peak remained unchanged with C_0, whereas those of the small and large micelles increased with increasing C_0 little and markedly, respectively.

Table 2 summarizes the literature values of m and R_h in dilute solution at 25 °C. These m values are very large, and consequently we can use the phase separation approximation, C_1=cmc. The simplest model which may apply to the results shown in Fig. 2 is the secondary aggregation model described in the Theoretical Basis section. Substitution of Eqs. 8 and 9 into Eq. 4 yields

$$\log[C_0(V_2-V_c)+\mathrm{cmc}(V_1-V_2)]=m_2\log[C_0(V_c-V_3)+\mathrm{cmc}(V_3-V_1)]+\log K-(m_2-1)\log(V_2-V_3) \quad (10)$$

The V_c value can be determined from both the leading and trailing boundaries of a frontal elution curve. Since these V_c values were close, we used the average of them. The centroid volumes, V_2 and V_3, of the small and large micelles are expected to be close to the corresponding peak volumes, V_{2p} and V_{3p}. The difference in V between the centroid and the peak stems from both asymmetry of the peak and the concentration dependence of the peak position. Furthermore V_1 should be close to V_c at infinite dilution, whereas V_3 should be close to V_c at infinite concentration. By employing values of V_1=35.5 cm^3, V_2=17.0 cm^3, V_3=9.5 cm^3, and cmc=0.06 mmol dm^{-3}, we plotted the V_c data on column A according to Eq. 10 in Fig. 3. By the least-squares method, we obtained values of m_2=6.04 and K_2=6.25 (mmol dm^{-3})$^{-5.04}$. From this m_2 value we can suggest that the large micelle of $C_{12}E_5$ is the hexamer of the small micelle.

Computer Simulation of GFC Patterns for $C_{12}E_5$. The computer simulation of GFC patterns based on plate theory has become a useful tool for investigating

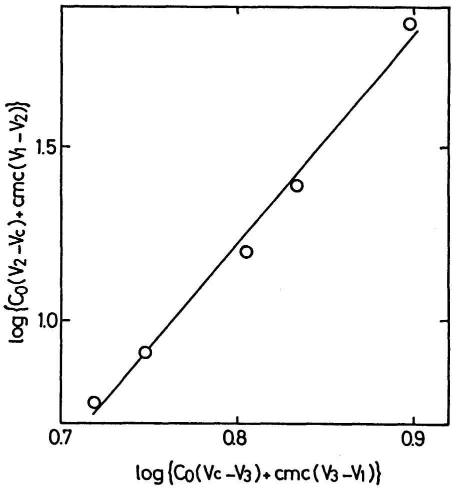

Fig. 3. Centroid volume data plotted according to Eq. 10 for $C_{12}E_5$ by using values of V_1=35.5 cm^3, V_2=17.0 cm^3, V_3=9.5 cm^3, and cmc=0.06 mmol dm^{-3}.

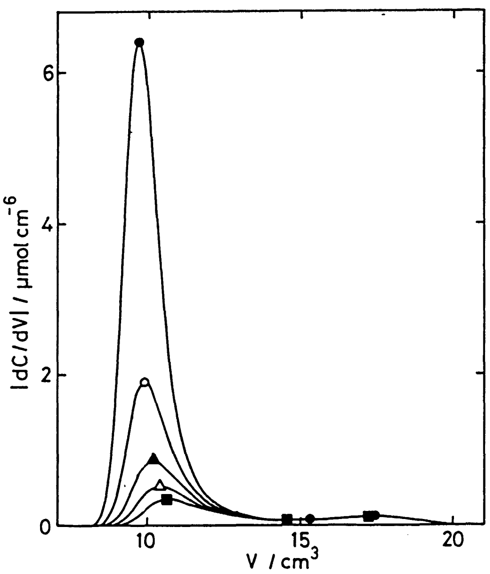

Fig. 4. Computer-simulated derivative patterns for $C_{12}E_5$ at the concentrations corresponding to Fig. 2. Input data used for the simulation: n=100, V_0=7.0 cm^3, V_1=35.5 cm^3, V_2=17.0 cm^3, V_3=9.5 cm^3, m_2=6, K_2=6.25 (mmol dm^{-3})$^{-5}$, and cmc=0.06 mmol dm^{-3}.

the aggregation properties of surfactants.[2,20,23] Taking into the literature m values (Table 2), we used values of m_1=500 and m_2=6. The elution volumes estimated above, V_1=35.5 cm^3, V_2=17.0 cm^3, and V_3=9.5 cm^3 were also used below. A K_1 value of 5×10^{606} (mmol dm^{-3})$^{-499}$ were estimated from the equation,[20] $K_1=\mathrm{cmc}^{1-m_1}/(2m_1)$, by using cmc=0.06 mmol dm^{-3} and m_1=500. A K_2 values of 6.25 (mmol dm^{-3})$^{-5}$ were used. As fitting parameters, we used V_0=7.0 cm^3 and n=100. Figure 4 shows the computer simulated GFC patterns of $C_{12}E_5$, corresponding to the experimental ones (Fig. 2). Very close patterns were obtained by using cmc=0.06 mmol dm^{-3} (phase separation model), without using the m_1 and K_1 values, though they are not shown.

In Fig. 4 two peaks for small and large micelles are reproduced. This result differs from that of $C_{12}E_6$; the GFC derivative patterns for $C_{12}E_6$ had only one peak for the micelle, and the micellar elution volume decreased markedly with increasing C_0.[2] These different patterns can be ascribed to the difference in m_2; m_2=6 for $C_{12}E_5$ and m_2=2 for $C_{12}E_6$. The computer simulations based on plate theory correspond to the experimental GFC patterns for these surfactants. Furthermore we recall that asymptotic theory predicts only one peak at m=2 and two peaks at $m\geqq3$ for the monomer-m-mer system.[20] For the small micelle, both the observed and simulated values of V_{2p} slightly increased with increasing C_0, but the height simulated is larger than the observed one. For the large micelle, the simulated V_{3p} value decreased with increasing C_0 more rapidly than the observed one. Considering the inaccuracies in both experiment and theory, we did not attempt further improvements of fitting.

The hydrodynamic radius R_h of a species can be estimated from its elution volume V_e by using a calibration relationship between R_h and V_e for the proteins described in the Experimental section. For the small micelle of $C_{12}E_5$, we obtained values of R_h=5.0 nm (C_0=1.531 mmol dm^{-3}, on column A) and R_h=5.3 nm (C_0=1.530 mmol dm^{-3}, on column B) from their V_{2p} values, and a value of R_h=4.9 nm from V_2=17.0 cm^3. For the large micelle of $C_{12}E_5$, we could not determine the R_h value from the Sephadex G-200 data,since V_{3p} and V_3 were close to the exclusion limit of R_h for this gel. By using column C (Sephacryl S-500), we estimated a value of R_h=30 nm (C_0=9.816 mmol dm^{-3}).

$C_{12}E_8$. For $C_{12}E_8$ at 25 °C, there is general agreement that the micelle size little changes with C_0.[1,3,6-13,16]

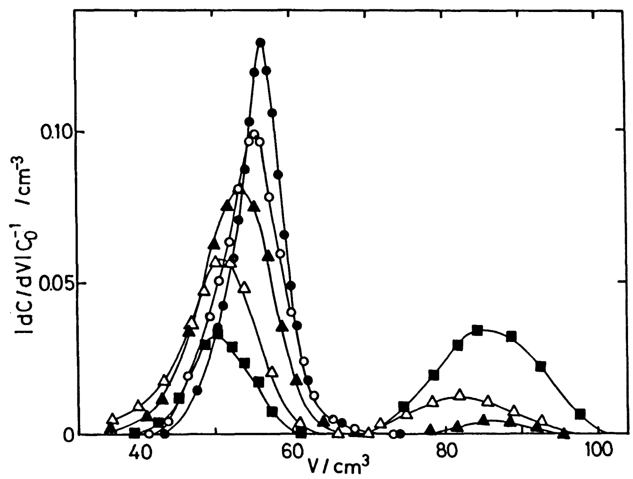

Fig. 5. Reduced derivative patterns for $C_{12}E_8$ at five charged concentrations (C_0/mmol dm^{-3}): 0.164 (■); 0.329 (△); 0.986 (▲); 21.655 (○); 42.336 (●).

Table 3 summarizes the literature values of m and R_h in dilute solution at 25 °C. The derivative patterns for $C_{12}E_8$ at the trailing boundary are shown in Fig. 5, where the ordinate is divided by C_0 for representing the GFC data in a wide range of C_0. As expected, there appeared a single peak of the micelle. As we have shown theoretically, the concentration dependence of the micellar peak V_{mp} is rather complicated;[24] when m is large enough, like $C_{12}E_5$, V_{mp} increases slightly with increasing C_0. The increase of V_{mp} shown in Fig. 5 is much larger than that predicted by plate theory. Furthermore the peak height of the micelle should be roughly proportional to C_0 at high concentrations, and consequently the peak divided by C_0 should have a constant height. As Fig. 5 shows, the micellar peak at C_0=42.336 mmol dm^{-3} is higher than that at C_0=21.655 mmol dm^{-3}. Though the reason has not yet been clarified, the peak position V_p sometimes increases with increasing C_0.[25] Then, as C_0 increases, the leading peak becomes broader, whereas the trailing peak becomes sharper.[20,26] These tendencies have been explained on the basis of plate theory for a nonassociable protein.[26] Values of cmc were reported to be 0.11[22] and 0.07 mmol dm^{-3}.[27]

Taking into consideration the above-mentioned results, we computer-simulated the derivative curve by using the following values; V_0=5.0 cm^3, V_1=83.8 cm^3, V_2=0.0822C_0+51.93 cm^3, and cmc=0.10 mmol dm^{-3}. The derivative patterns thus computed are shown by dashed lines. The solid lines were computed by using the mass action model; values of m=100 and K=4.9×10^{96} (mmol dm^{-3})$^{-99}$ were used instead of the cmc value (phase separation model). Though the difference between the solid and dashed lines is minor, the solid line is closer to the observed value than the dashed line. These computed patterns well reproduce the observed results (Fig. 5). Therefore, the increase of the micellar elution volume does not reflect true changes in micelle size.

The R_h value for the $C_{12}E_8$ micelle might be estimated to be 3.8 nm from the V_{2p} value at C_0=42.336 mmol dm^{-3}. For the monomer-m-mer system we have shown that the elution volume at infinite concentration corresponds to the true R_h value for the m-mer.[24] Therefore "true" R_h value for the $C_{12}E_8$ micelle may be smaller than 3.8 nm, as have been reported by other workers (Table 3).

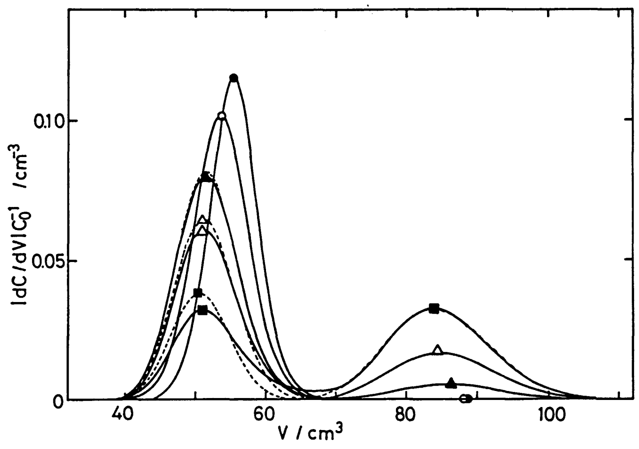

Fig. 6. Computer-simulated reduced derivative patterns for $C_{12}E_8$ at the five concentrations corresponding to Fig. 5. Input data used for the simulation according to two models: for mass action model (solid lines), n=120, V_0=5.0 cm^3, V_1=83.8 cm^3, V_2=0.0822C_0+51.93 cm^3, m=100, and K=4.9×10^{96} (mmol dm^{-3})$^{-99}$; for phase separation model (dashed lines), cmc=0.10 mmol dm^{-3} and the same values of n, V_0, V_1, and V_2.

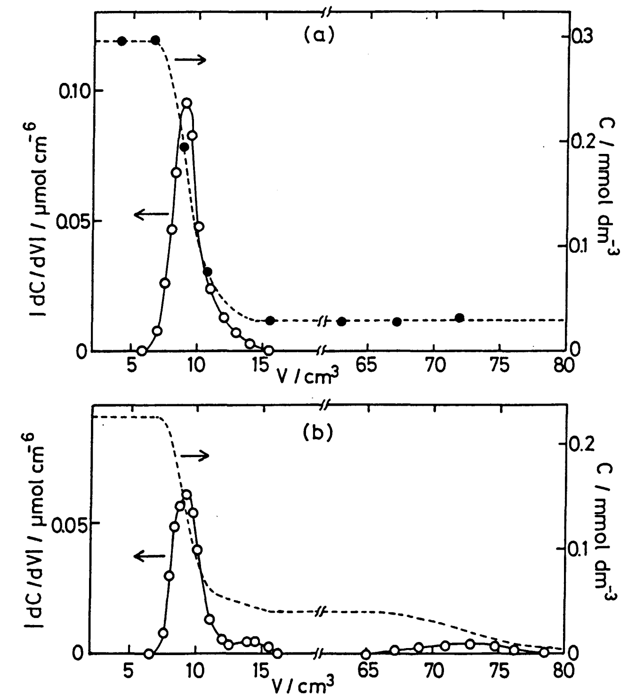

Fig. 7. Elution curves (dashed lines) and their derivatives (solid lines) for $C_{12}E_4$ under two experimental conditions: column D and C_0=0.508 mmol dm^{-3} (a); column C and C_0=0.276 mmol dm^{-3} (b).

$C_{12}E_4$. For $C_{12}E_4$ at 25 °C, values of cmc=0.04,[28] 0.046,[16] and 0.064[22] mmol dm^{-3} and R_h=180 nm (SLS)[29] have been reported. On two columns, columns C and D, we investigated the GFC patterns of $C_{12}E_4$. In the elution pattern of this surfactant, the concentration at the first plateau region was smaller than the initially charged concentration C_0, as shown in Figs. 7a (Sephadex G-200) and 7b (Sephacryl S-500). For the both columns the concentration at the second plateau region was close to the cmc and the V_1 value was much larger than the V_t value (Table 1). The latter fact indicates that the $C_{12}E_4$ monomer is adsorbed on the gels. This adsorption is ascribed to the hydrophobicity of $C_{12}E_4$. The reason for the reduction of concentration in eluate below C_0 may be ascribed to the adsorption or the clogging of huge micelles of $C_{12}E_4$ to the gel network. On Sephacryl S-500, the large peak appeared near the void volume

Table 3. Aggregation Numbers and Hydrodynamic Radii of $C_{12}E_8$ Micelles in Dilute Solution at 25 °C

C / mmol dm^{-3}	m	R_h / nm	Method	Reference
cmc	120	3.6	SV	1
cmc		3.5	GFC, VIS	1
8.2	97		GFC, SLS	3
cmc	62	2.8	SLS, VIS	6
cmc	120	3.4	SLS, DLS	7
cmc	90	3.0	SLS, NMR	8
9.3		3.3	NMR	9
cmc		3.1	NMR	10
2.5%	90	3.1	SNS, DNS	11
28	82	3.0	SNS	12
7	92		FD	13
3%	105		FQ	13
cmc	39		VPO	16
42.34		3.8[a]	GFC	This work

a) Estimated from the micellar peak shown in Fig. 5. The "true" value is expected to be smaller.

(Table 1) and the small peak has a value of R_h=33 nm. On Sephadex G-200, a single peak appeared near the void volume of this column, since all micelles of $C_{12}E_4$ are too large as compared with the gel pores.

Micellar Growth of Polyethylene Glycol Dodecyl Ethers at 25 °C. As Table 2 shows, VPO and EPR data on $C_{12}E_5$ have been interpreted as showing that small micelles form independently of C_0 above the cmc.[14,16] On the other hand, the NMR and SLS data (Table 2) suggested that large micelles form and grow with increasing C_0.[4,5,8-10] A similar controversy continues for $C_{12}E_6$.[2]

Our present and previous researches clearly showed that micellar size of $C_{12}E_4$, $C_{12}E_5$, $C_{12}E_6$, and $C_{12}E_8$ increases with a decrease of the polyoxyethylene chain length and with increasing C_0 except for $C_{12}E_8$ this result is consistent with others.[1,3,6-13,16] However our result on $C_{12}E_8$ does not show that smaller micelles do not form at very low concentrations, especially near the cmc. Very small m values have been reported, as shown in Table 3.[6,16] This discrepancy in m may stem from the difference in the extrapolation procedure of low concentration data to the cmc.

Our GFC data on $C_{12}E_5$ clearly indicate that small micelles coexist with large micelles. This result was analyzed in terms of the secondary aggregation model, viz., by assuming that sizes of these micelles are independent of C_0. This assumption may be valid in the concentration range which we investigated (C_0= 1.53—10.4 mmol dm^{-3}). Outside this range, smaller or larger micelles may form.

The molecular lengths of $C_{12}E_4$, $C_{12}E_5$, and $C_{12}E_8$ in the most stretched conformation are 3.2 nm, 3.5 nm, and 4.4 nm, respectively. From comparison between these values and R_h's, the $C_{12}E_8$ micelle is almost spherical and all the $C_{12}E_4$ and $C_{12}E_5$ micelles are nonspherical (probably rodlike).

The most important conclusion in this work is that the small and large micelles coexist for $C_{12}E_4$ and $C_{12}E_5$.

List of Symbols.

C_0; Total concentration of surfactant on a monomer basis
C_1; Monomer concentration of surfactant
C_2; Concentration of small micelles on a monomer basis
C_3; Concentration of large micelles on a monomer basis
K_1; Equilibrium constant of formation of small micelles from monomers
K_2; Equilibrium constant of formation of large micelles from small micelles
m; Number of monomers in a micelle
m_1; Number of monomers in a small micelle
m_2; Number of small micelles in a large micelle
n; Number of plates or number of oxyethylene units
V_0; Void volume
V_1; Centroid elution volume of monomers
V_2; Centroid elution volume of small micelles
V_3; Centroid elution volume of large micelles
V_c; Overall centroid elution volume
V_t; Total volume of gel bed
V_{1p}; Peak position of monomers in the derivative pattern
V_{2p}; Peak position of small micelles in the derivative pattern
V_{3p}; Peak position of large micelles in the derivative pattern

Thanks are due to Ms. M. Abe for technical assistance.

References

1) C. Tanford, Y. Nozaki, and M. F. Rohde, *J. Phys. Chem.*, **81**, 1550 (1977).
2) N. Funasaki, S. Hada, and S. Neya, *J. Phys. Chem.*, **92**, 3488 (1988) and references cited therein.
3) S. Maezawa, Y. Hayashi, J. Ishii, K. Kameyama, and T. Takagi, *Biochim. Biophys. Acta*, **747**, 291 (1983).
4) N. Nishikido, M. Shinozaki, G. Sugihara, and M. Tanaka, *J. Colloid Interface Sci.*, **82**, 352 (1981).
5) M. Okawauchi, M. Shinozaki, Y. Ikawa, and M. Tanaka, *J. Phys. Chem.*, **91**, 109 (1987).
6) T. Sato, Y. Saito, and I. Anzai, *J. Chem. Soc., Faraday Trans. 1*, **84**, 275 (1988).
7) M. Corti, C. Minero, and V. Degiorgio, *J. Phys. Chem.*, **88**, 309 (1984).
8) W. Brown, Z. Pu, and R. Ryahen, *J. Phys. Chem.*, **92**, 6086 (1988).
9) T. Kato, S. Anzai, S. Takano, and T. Seimiya, Proceedings of the 39th Sympsium on Colloid and Interface Chemistry, the Chemical Society of Japan (1986), p. 160.
10) P. G. Nilsson, H. Wennerström, and B. Lindman, *J. Phys. Chem.*, **87**, 1377 (1983).
11) M. Zulauf, K. Weckström, J. B. Hayter, V. Degiorgio, and M. Corti, *J. Phys. Chem.*, **89**, 3411 (1985).
12) L. Magid, R. Triolo, and J. S. Johnson, Jr., *J. Phys. Chem.*, **88**, 5730 (1984).
13) W. Binana-Limbele and R. Zana, *J. Colloid Interface Sci.*, **121**, 81 (1988).
14) J. M. DiMeglio, L. Paz, M. Dvolaitzky, and C. Taupin, *J. Phys. Chem.*, **88**, 6036 (1984).
15) D. O. Lasic, *J. Colloid Interface Sci.*, **113**, 188 (1986).
16) T. M. Herrington and S. S. Sahi, *J. Colloid Interface Sci.*, **121**, 107 (1988).

17) P. G. Nesson and R. Jennings, *Faraday Discuss. Chem. Soc.,* **76**, 353 (1983).
18) J. M. Corkill, J. F. Goodman, T. Walker, and J. Wyer, *Proc. R. Soc. London, Ser.* A, **312**, 243 (1969). P. Mukerjee, *J. Phys. Chem.*, **76**, 565 (1972). R. J. M. Tausk and J. Th. G. Overbeek, *Biophys. Chem.*, **2**, 175 (1974). P. J. Missel, N. A. Mazer, G. B. Benedek, C. Y. Young, and M. C. Carey, *J. Phys. Chem.*, **84**, 1044 (1980). E. Y. Sheu, S.-H. Chen, and J. S. Huang, *J. Phys. Chem.*, **91**, 3306 (1987).
19) P. H. Elworthy and C. B. MacFarlane, *J. Chem. Soc.*, **1963**, 907. S. Ikeda, "Surfactants in Solution," ed by K. L. Mittal and B. Lindman, Vol. 2, Plenum, New York (1984), p. 825. T. Imae, R. Kamiya, and S. Ikeda, *J. Colloid Interface Sci.*, **108**, 215 (1985). S. Ikeda, S. Ozeki, and K. Kakiuchi, *J. Phys. Chem.*, **92**, 3465 (1988). G. Porte, Y. Poggi, J. Appell, and G. Maret, *ibid.*, **88**, 5713 (1984). W. H. Richtering, W. Burchard, E. Jahns, and H. Finkelmann, *ibid.*, **92**, 6032 (1988).
20) N. Funasaki, S. Hada, and S. Neya, *Bull. Chem. Soc. Jpn.*, **62**, 380 (1989).
21) H. Lange, *Kolloid Z.*, **201**, 131 (1965).
22) M. J. Rosen, A. W. Cohen, M. Dahanayake, and X. Hua, *J. Phys. Chem.*, **86**, 541 (1982).
23) T. Nakagawa, *Yukagaku*, **20**, 277 (1971).
24) N. Funasaki, S. Hada, and S. Neya, *Bull. Chem. Soc. Jpn.*, **61**, 2961 (1988).
25) G. K. Ackers, *Adv. Protein Chem.*, **24**, 343 (1970).
26) D. J. Winzor and L. W. Nichol, *Biochim. Biophys. Acta*, **104**, 1 (1965).
27) K. Meguro, Y. Takasawa, N. Kawahashi, Y. Tabata, and M. Ueno, *J. Colloid Interface Sci.*, **83**, 50 (1981).
28) M. J. Schick, *J. Colloid Sci.*, **17**, 801 (1962).
29) H. Hoffmann, H. S. Kielman, D. Pavlovic, and G. Platz, *J. Colloid Interface Sci.*, **80**, 237 (1981).